HHS Public Access

Author manuscript

J Am Coll Cardiol. Author manuscript; available in PMC 2014 December 24.

Published in final edited form as:

J Am Coll Cardiol. 2013 December 24; 62(25): 2395–2403. doi:10.1016/j.jacc.2013.08.715.

Comparative electromechanical and hemodynamic effects of left ventricular and biventricular pacing in dyssynchronous heart failure: *electrical resynchronization versus left-right ventricular interaction*

Joost Lumens, PhD[*,†], **Sylvain Ploux, MD**[*,†], **Marc Strik, MD**[†], **John Gorcsan III, MD**[‡], **Hubert Cochet, MD**[*], **Nicolas Derval, MD**[*], **Maria Strom, PhD**[§], **Charu Ramanathan, PhD**[§], **Philippe Ritter, MD**[*], **Michel Haïssaguerre, MD**[*], **Pierre Jaïs, MD**[*], **Theo Arts, PhD**[†], **Tammo Delhaas, MD,PhD**[†], **Frits W. Prinzen, PhD**[†], and **Pierre Bordachar, MD,PhD**[*]

[*]Hôpital Cardiologique du Haut-Lévêque, CHU Bordeaux, L'Institut de rythmologie et modélisation cardiaque (LIRYC), Université Bordeaux, Bordeaux, France [†]Maastricht University Medical Center, Cardiovascular Research Institute Maastricht (CARIM), Maastricht, The Netherlands [‡]University of Pittsburgh, Pittsburgh, PA [§]CardioInsight Technologies, Cleveland, OH

Abstract

Objectives—To enhance understanding of the working mechanism of cardiac resynchronization therapy (CRT) by comparing animal experimental, clinical, and computational data on the hemodynamic and electromechanical consequences of left ventricular and biventricular pacing (LVP and BiVP, respectively).

Background—It is unclear why LVP and BiVP have comparative positive effects on hemodynamic function of patients with dyssynchronous heart failure (HF).

Methods—Hemodynamic response to LVP and BiVP (%-change $LVdP/dt_{max}$) was measured in 6 dogs and 24 patients with HF and left-bundle branch block (LBBB), followed by computer simulations of local myofiber mechanics during LVP and BiVP in the failing heart with LBBB. Pacing-induced changes of electrical activation were measured in dogs using contact mapping and in patients using a noninvasive multielectrode electrocardiographic mapping technique.

Address for correspondence: Joost Lumens, PhD, Maastricht University Medical Center, Cardiovascular Research Institute Maastricht (CARIM), Universiteitssingel 50, P.O. Box 616, 6200MD Maastricht, The Netherlands, joost.lumens@maastrichtuniversity.nl, Tel: +31433881659, Fax: +31433881725.

DISCLOSURES: P. Jaïs and M. Haïssaguerre are stock owners of CardioInsight Technologies Inc (Cleveland, OH). F.W. Prinzen has received research grants from Medtronic (Minneapolis, MN), EBR Systems (Sunnyvale, CA) and MSD (Whitehouse Station, NJ). J. Gorcsan has received research grants from Biotronik (Berlin, Germany), Medtronic (Minneapolis, MN), St. Jude Medical (Sylmar, CA), and is a consultant for CardioInsight Technologies Inc (Cleveland, OH). M. Strom and C. Ramanathan are paid employees and stock owners of CardioInsight Technologies Inc (Cleveland, OH).

Results—LVP and BiVP similarly increased $LVdP/dt_{max}$ in dogs and in patients, but only BiVP significantly decreased electrical dyssynchrony. In the simulations, LVP and BiVP increased total ventricular myofiber work to the same extent. While the LVP-induced increase was entirely due to enhanced right ventricular (RV) myofiber work, the BiVP-induced increase was due to enhanced myofiber work of both the LV and RV. Overall, $LVdP/dt_{max}$ correlated better with total ventricular myofiber work than with LV or RV myofiber work alone.

Conclusions—Experimental, human, and computational data support the similarity of hemodynamic response to LVP and BiVP, despite differences in electrical dyssynchrony. The simulations provide the novel insight that, through ventricular interaction, the RV myocardium importantly contributes to the improvement in LV pump function induced by CRT.

Keywords

ventricular interaction; myocardial work; cardiac resynchronization therapy; dyssynchrony; electrophysiology mapping

INTRODUCTION

Cardiac resynchronization therapy (CRT) is an effective treatment for patients with chronic heart failure (HF), decreased left ventricular (LV) ejection fraction (≤35%), and left bundle-branch block (LBBB) (1, 2). Its working action is generally believed to originate from resynchronization of LV and right ventricular (RV) electrical activation, achieved by biventricular pacing (BiVP).

Paradoxically, single-site LV pacing (LVP) has been shown to be as beneficial as BiVP for LV systolic pump function in acute hemodynamic studies (3–5), in long-term follow-up studies (6–8), and even in situations where LVP is unlikely to result in fusion of two activation wavefronts induced by LVP and intrinsic conduction (5, 9). Therefore, the question arises whether electrical resynchronization is the primary working mechanism underlying the functional improvement induced by CRT. It is well known that ventricular pacing redistributes mechanical work in the LV wall so that the region of latest activation is associated with highest mechanical work (10). It is, however, not known to what extent ventricular pacing affects mechanical work generated by the RV myocardium. Since direct mechanical coupling of the ventricles allows transmission of myocardial work between the ventricles, we hypothesize that pacing-induced increase of RV myocardial work can benefit LV pump function.

In order to test this hypothesis, we measured local electrical and global hemodynamic function in an animal model of chronic HF with LBBB and in CRT candidates during baseline (LBBB), LVP, and BiVP. Furthermore, we used a computer model of the human heart and circulation (11–13) to investigate the consequences of LVP and BiVP for local LV and RV tissue mechanics. Together, these complementary data provide novel insights in the working mechanism of CRT, especially the involvement of the RV myocardium in its hemodynamic effect.

METHODS

ANIMAL EXPERIMENTS

Animal handling was performed according to the Dutch Law on Animal Experimentation and the European Directive for the Protection of Vertebrate Animals used for Experimental and Other Scientific Purposes (86/609/EU). The protocol was approved by the Experimental Animal Committee of Maastricht University.

In 6 adult mongrel dogs (29±3 kg), LBBB was induced by radiofrequency ablation and, subsequently, HF was induced by 4 weeks of tachypacing (14). Continuous, invasive hemodynamic and electrocardiographic measurements were performed during right atrial pacing at approximately 10 bpm above intrinsic heart rate (baseline) and during atrial paced LVP and BiVP at the same heart rate and short atrioventricular (AV) delay ensuring full ventricular capture as noticed on the surface electrocardiogram (ECG). More details of the experimental protocol are provided in Online Supplement A.

Electrical activation maps were used to calculate two indices of electrical dyssynchrony, i.e., total ventricular activation time (AT_{TOT}) derived from all electrodes and LV activation time (AT_{LV}) derived from the septal and LV free wall electrodes only (14).

PATIENT MEASUREMENTS

The execution of the study conformed to the principles outlined in the Declaration of Helsinki on research in human subjects. The study protocol was approved by the Medical Ethics Committee of CHU Bordeaux. All patients granted their written approval to participate in the study.

Patient population—The study included 24 consecutive patients who fulfilled the following criteria: 1) New York Heart Association (NYHA) functional class II, III, or IV despite optimal medical therapy, 2) LV ejection fraction ≤ 35% during sinus rhythm, 3) QRS duration ≥120ms, and 4) LBBB morphology on the surface ECG. Both, QRS duration and LBBB morphology were defined according to the most recent AHA/ACCF/HRS recommendations (15). Etiology was considered ischemic in the presence of significant coronary artery disease (≥50% stenosis in one or more of the major epicardial coronary arteries), history of myocardial infarction, or prior revascularization.

Device implantation, pacing protocol, and assessment of hemodynamic function—All patients were implanted with a CRT device with leads in the RV apex and in a lateral or posterolateral branch of the coronary sinus. Within 72 hours after device implantation, a high-fidelity pressure-recording micromanometer (Radi Medical Systems; St Jude Medical, St. Paul, MN) was introduced in the LV cavity. LV pressure data were acquired (16) during baseline (AAI mode; 10 bpm above intrinsic heart rate) and during atrial paced LV and BiV stimulation (DDD mode). The AV delay was set to the longest delay that did not lead to fusion between electrical activation waves originating from intrinsic RV conduction and from the LV pacing electrode during LVP. The same AV delay was used during BiVP with simultaneous LV-RV stimulation. Hemodynamic response was defined as %-change in maximal rate of LV pressure rise ($LVdP/dt_{max}$) relative to baseline.

Noninvasive electrocardiographic mapping—In a subset of 10 patients, we used noninvasive, high-resolution electrocardiographic mapping (ECM; CardioInsight™ Technologies Inc, Cleveland, Ohio) to acquire ventricular epicardial activation maps during baseline, LVP, and BiVP (17, 18) and to quantify electrical dyssynchrony (AT_{TOT} and AT_{LV}).

SIMULATIONS

The CircAdapt model of heart and circulation (11, 19) was used to quantify the acute effects of LVP and BiVP on ventricular mechanics and hemodynamics of the failing heart with LBBB. The model consists of modules representing cardiac walls, cardiac valves, large blood vessels, systemic and pulmonary peripheral vasculature, the pericardium, and local cardiac myofiber mechanics (Online Supplement B). It enables realistic beat-to-beat simulation of cardiovascular mechanics and hemodynamics under a wide variety of (patho-)physiological circumstances, including ventricular mechanical dyssynchrony (12, 13).

First, mechanics and hemodynamics of the normal cardiovascular system with nonfailing myocardium and synchronous activation of the ventricular walls were simulated as published previously (12, 13). Second, a failing heart with LBBB was simulated (Online Supplement C). Third, LVP and BiVP were simulated so that they were in agreement with the electrocardiographic mapping data obtained in the patients and dogs, i.e., LVP did not change AT_{TOT} (135 ms), whereas BiVP was assumed to reduce AT_{TOT} from 135 to 60 ms (Online Supplement C).

Local ventricular myofiber mechanics—Simulated time courses of local Cauchy myofiber stress and natural strain were used to quantify regional differences in mechanical load and deformation of the myocardial tissue during LBBB, LVP and BiVP. Peak systolic myofiber stress and external myofiber work were quantified as indices of local myocardial tissue load. External myofiber work, expressed in joule per cardiac cycle (J/beat), was defined as the area enclosed by the stress-strain relation multiplied by tissue volume of the myocardial segment, which equaled 8.5 mL for each ventricular wall segment.

STATISTICAL ANALYSIS

Values are presented as mean ± standard deviation (SD) for continuous variables and as numbers and percentages for discrete variables. Statistical analysis was performed with the IBM SPSS Statistics 20 package for Windows (IBM Corp., Armonk, NY). Assumptions on homogeneity of variances and normality of residual distributions were checked using Mauchly's test of sphericity and Q-Q plots, respectively. One-way repeated measures analysis of variance (ANOVA) was used to test for significant effects of LVP and BiVP on baseline electrical and hemodynamic function parameters. If the sphericity assumption appeared to be violated, the Greenhouse–Geisser correction was used to adjust degrees of freedom for the averaged results of the ANOVA. In case ANOVA showed significance, pairwise post-hoc analysis for differences between the three pacing conditions (no pacing/LVP/BiVP) was performed using Fisher's Least Significant Difference method. A *p*-value <0.05 was considered statistically significant for all analyses.

RESULTS

DOGS AND PATIENTS

Baseline conditions of dogs and patients are presented in Tables 1 and 2, respectively. Paced AV delay was relatively short compared to the PR interval in dogs (86±26 versus 141±40 ms, respectively) as well as in patients (106±19 versus 213±30 ms).

LVP and BiVP similarly improve systolic LV function—Both LVP and BiVP similarly increased $LVdP/dt_{max}$ compared to baseline in dogs (LVP versus BiVP: 21±19 versus 19±17%, p=0.33; Table 1) and patients (16±13 versus 16±11%, p=0.95; Table 3). Animal experimental data showed a trend toward increased LV stroke volume, pump stroke work, and systolic peak pressure during LVP and BiVP as compared to baseline, while LV end-diastolic volume and pressure remained unchanged (Table 1). In contrast, RV systolic peak pressure and $RVdP/dt_{max}$ were decreased during LVP as compared to baseline and BiVP.

BiVP but not LVP reduces electrical dyssynchrony—Ventricular electrical activation maps of dogs and patients revealed the same characteristics (Figure 1): during baseline a classical LBBB-pattern of electrical activation starting at the lateral RV free wall and gradually spreading towards the lateral LV free wall; during LVP a mirrored LV-to-RV pattern of epicardial activation; and during BiVP two fusing wavefronts of activation originating from the LV and RV pacing sites. In addition, the dog data showed that the septum is activated in RV-to-LV transmural direction during baseline and BiVP, and in LV-to-RV direction during LVP. Compared to baseline, BiVP significantly reduced electrical dyssynchrony in dogs and in patients (Figure 2), whereas LVP did not. In the dogs, activation times were significantly smaller during BiVP than during LVP (Table 1). In the patients, only AT_{TOT} was significantly smaller during BiVP than during LVP (Table 3).

SIMULATIONS

Also the model simulations showed that LVP and BiVP similarly increased $LVdP/dt_{max}$ by 15% (Table 4), despite the longer ventricular activation time during LVP. As in the dogs, both pacing strategies increased LV stroke volume, pump stroke work, and systolic peak pressure (Table 4) and LVP decreased $RVdP/dt_{max}$ compared to baseline. In addition, simulations revealed that both LVP and BiVP increased RV pump stroke work by 16%.

LVP and BiVP differently affect local ventricular myofiber mechanics—Pronounced local differences are present in the pattern and amplitude of myofiber strain during baseline (LBBB), LVP, and BiVP (Figure 3). Early-activated segments are characterized by rapid onset of systolic myofiber shortening followed by rebound stretch and in some cases a second phase of shortening at the end of systole. In late-activated regions, early-systolic stretch is followed by pronounced systolic myofiber shortening.

The regional differences in strain patterns translated into differences in local mechanical tissue load (Figure 3: color maps). In the LBBB simulation, most mechanical myofiber work was generated by the LV free wall segments, whereas the RV free wall and septal segments

generated little mechanical work or even dissipated mechanical work as evidenced by the clockwise stress-strain relations (Figure 3). Compared to LBBB, LVP reallocated mechanical work from the LV free wall to the septum, resulting in a spatially mirrored but equally dispersed distribution of mechanical work over the LV myocardium. BiVP was associated with less early-systolic myofiber stretch and shortening and a more homogeneous distribution of myofiber work than LVP (Figure 3). In contrast, LV peak systolic myofiber stress was more homogeneously distributed during LVP, whereas the average values did not differ between LVP and BiVP (92±7 and 92±13 kPa, respectively).

LBBB and LVP were associated with a comparable net amount of mechanical myofiber work generated by the LV myocardium (Figure 4). The RV myocardium, however, generated more work during LVP than during LBBB. As a result, LVP acutely increased total ventricular myofiber work by 25%. BiVP resulted in similar increase of total myofiber work (23%) as LVP, but now due to an increase of both LV and RV myofiber work.

Ventricular interaction: contribution of RV myocardium to LV pump function— A more precise study on the role of left-right ventricular interaction on hemodynamic response to pacing therapy was performed by simulating LVP and BiVP with five different AV delays (60/80/100/120/140 ms) as well as five different velocities of activation, that resulted in a range of values for AT_{TOT} (24/36/48/60/72 ms during BiVP and 54/81/108/135/162 ms during LVP). For the resulting 50 simulations, Figure 5 shows the relationship between ventricular myofiber work and $LVdP/dt_{max}$. The left panel indicates that total ventricular myofiber work increased linearly with $LVdP/dt_{max}$ and that this linear relationship was virtually independent of the pacing mode. However, LVP and BiVP behaved differently when considering LV and RV myofiber work separately (middle and right panel of Figure 5respectively). While LVP and BiVP can lead to the same total ventricular myofiber work and $LVdP/dt_{max}$, the contribution of LV myofiber work is smaller and that of RV myofiber work is larger during LVP. During BiVP, the relative contribution of the RV myocardium to total ventricular myofiber work was rather constant and ranged from 22 to 24%. This contribution was considerably more variable during LVP and increased from 28% in the simulation with highest conduction velocity to 38% in that with lowest. Overall, these simulation data highlight the important role of the RV myocardium as contributor to LV pump function during LVP and thus the importance of ventricular interaction during CRT.

DISCUSSION

In the present study, we demonstrate that LVP and BiVP improve systolic function of the dyssynchronous failing heart to a similar extent, both in experimental animals and in patients. With state-of-the-art techniques for electrical mapping, we showed for the first time in patients that pacing-induced hemodynamic improvement can occur without electrical resynchronization. These findings are corroborated by computer simulations, showing that both pacing strategies increase total ventricular myofiber work to a similar extent, yet differently redistribute myofiber load over the LV and RV myocardium. Overall, LV systolic function correlates better with total rather than with LV or RV myofiber work alone.

These data provide the novel insight that left-right ventricular interaction is an important determinant of the hemodynamic effect of pacing therapy in dyssynchronous HF.

RV mechanical work: the missing link in the explanation for similarity of response to LVP and BiVP?

Our finding that LVP and BiVP improve LV systolic function to the same extent corroborates previously published data on acute hemodynamic response (3, 4) and on long-term clinical response and reverse remodeling (6–8). In addition, the present study provides a potential mechanism underlying these observations.

It is known that contractile harmony is substantially disturbed in patients with LBBB or pacing-induced electrical dyssynchrony and that this contractile discordance compromises cardiac pump function. Regional differences in the systolic deformation pattern are related to local differences in sarcomere length and, consequently, myofiber contractile force (20) and work load (10). The simulations are in close agreement with experimental findings demonstrating that mechanical myofiber work is small or even negative in regions close to the pacing site and large in regions remote from the pacing site (10). So far, these insights remained limited to the LV wall. Our simulations show for the first time that the RV myocardium contributes significantly to the improvement of LV pump function in pacing therapies, especially LVP. While it may be intuitive that BiVP improves LV pump function by increasing LV myofiber work, it may be less intuitive that LVP similarly improves LV systolic pump function by exclusively increasing the amount of mechanical work generated by the RV myocardium. These findings emphasize the importance of ventricular interaction, i.e., the property that the RV myocardium contributes to LV systolic pump function and vice versa.

Simulations of LVP and BiVP in hearts with different conduction velocities (Figure 5) revealed that, during LVP, the relative contribution of RV myofiber work to total ventricular myofiber work increased with total ventricular activation time, whereas it stayed constant during BiVP. These simulation data suggest that LVP is less effective than BiVP in patients with slow intramyocardial conduction, diminished RV contractile function, or in whom mechanical ventricular interaction is being impeded.

While indirect hemodynamic interaction results from the series coupling of the ventricles via the pulmonary and systemic circulations, direct mechanical interaction is due to the anatomical coupling via the interventricular septum and the surrounding pericardium (21). Since our animal experiments show no direct effect of LVP on indices of LV filling, such as LV end-diastolic pressure and volume (Table 1), the positive effect of LVP on LV systolic pump function most probably results from direct mechanical interaction. Furthermore, the decreased values of RV systolic pressure and $RVdP/dt_{max}$ with LVP suggest that the extra amount of mechanical work generated by the RV myocardium is largely converted into LV pump work through direct mechanical interaction.

Clinical implications and future perspectives

The demonstration that, during CRT, the RV myocardium can contribute to LV pump function and that this contribution differs between LVP and BiVP may explain why some

patients respond better to LVP and others to BiVP, as demonstrated in the GREATER EARTH study (6). We hypothesize that local differences in myocardial contractility (e.g., due to infarction, hibernation, etc.) determine a patient's response to LVP and BiVP in a way that hemodynamic improvement is compromised when the region with impaired contractile function coincides with the location of latest activation and, hence, highest mechanical load. Although experimental data point in this direction (22), it remains to be confirmed with prospective clinical studies.

Many studies demonstrated the acute deleterious effect of RV pacing on LV systolic function, in terms of $LVdP/dt_{max}$ (3, 4). Similarly, our experimental and simulation data revealed that LVP acutely decreased $RVdP/dt_{max}$ (Tables 1 and 4). Our simulations, however, additionally showed that RV pump stroke work was increased during both LVP and BiVP (Table 4). Therefore, it is questionable whether the pacing-induced decrease of $RVdP/dt_{max}$ should be considered as a sign of acute RV systolic impairment. At the same time, our simulations also showed that LVP increased mechanical myofiber work of the RV myocardial tissue by more than 100% (Figure 4). Whether this acute LVP-induced increase of RV tissue load translates into compensatory RV remodeling and eventually RV decompensation and failure, remains unknown and should be subject of future research.

Study limitations

In the present study, we evaluated the acute hemodynamic effect of CRT. Whether the observed acute hemodynamic improvements will evolve in chronic response to CRT, in terms of hard clinical endpoints or reverse remodeling, is unclear and should be subject of future research.

In dogs and patients, LVP and BiVP were applied with atrial pacing at short AV delay to ensure a constant heart rate and the absence of fusion between electrical activation waves originating from intrinsic conduction and from pacing electrode(s). These conditions have been chosen to clearly show the proof of principle that a pacing-induced hemodynamic benefit can be obtained in the absence of fusion in the case of LVP. Hence, our study is conceptually different from a previous study showing noninferiority of fusion-synchronized LVP compared to conventional simultaneous BiVP (23). We acknowledge that the AV delays used in this study may not have been the ones leading to optimal LV filling or systolic function. In a previous acute hemodynamic study (3), however, maximal aortic systolic or pulse pressure were observed at an AV delay of approximately 0.5x(PR interval-30 ms) for both LVP and BiVP. Applying this formula to our patient data, we obtained a predicted optimal AV delay of 92±15 ms, which is close to the AV delay programmed in this study (106±19 ms). Furthermore, the average paced AV delay in the patients was in good agreement with the value reported by Thibault *et al.* in the GREATER-EARTH study (101±16 ms), a study that also compared the effectiveness of LVP and BiVP in a conventional CRT population (7).

The multimodality of our study approach may have complicated interpretation of the results. At the same time, however, the consistency of hemodynamic and electrocardiographic response to LVP and BiVP in animals, patients, and simulations firmly evidenced that electrical resynchronization is not always required for pacing therapy to improve systolic

cardiac pump function. The invasive ECM data obtained in the dogs served as a control technique for our clinical ECM data obtained by noninvasive indirect mapping of epicardial electrical activation. The animal experimental protocol also included measurement of RV pressure data. These data enabled evaluation of the effects of LVP and BiVP on RV systolic function. The simulation data on RV function showed good agreement with the experimental data, i.e., LVP is associated with lower $RVdP/dt_{max}$ than BiVP.

Moreover, the computational model used in this study inherently provides a simplified representation of an average patient's failing heart with LBBB. Therefore, the conclusions drawn from these data should be interpreted with care. However, many model predictions agreed with measurements in patients and experimental animals. Moreover, the simplifications used allow a transparent view on complex fundamental mechanisms, which are hard to assess in experimental or clinical settings.

CONCLUSIONS

LVP and BiVP improve LV hemodynamic function to the same extent, despite substantial differences in electrical dyssynchrony. Both pacing strategies similarly increase total ventricular myofiber work, which is tightly linked to LV pump function. Our simulations show that CRT can improve LV systolic function by mechanical recruitment of the RV myocardium.

Supplementary Material

Refer to Web version on PubMed Central for supplementary material.

Acknowledgments

FUNDING SOURCES: This research was performed within the framework of CTMM, the Center for Translational Molecular Medicine (www.ctmm.nl), project COHFAR (grant 01C-203) cofunded by the Dutch Heart Foundation. J. Lumens received a grant within the framework of the Dr E. Dekker program of the Dutch Heart Foundation (NHS-2012T010). S. Ploux was financially supported by "la Fédération Française de Cardiologie". The study was also supported by the French Government, Agence National de la Recherche au titre du programme Investissements d'Avenir (ANR-10-IAHU-04).

Abbreviations and Acronyms

AT_{LV}	left ventricular activation time
AT_{TOT}	total ventricular activation time
BiVP	biventricular pacing
CRT	cardiac resynchronization therapy
HF	heart failure
LBBB	left bundle-branch block
LV	left ventricle/ventricular
LVP	left ventricular pacing

RV right ventricle/ventricular

REFERENCES

1. Abraham WT, Fisher WG, Smith AL, et al. Cardiac resynchronization in chronic heart failure. N Engl J Med. 2002; 346:1845–1853. [PubMed: 12063368]
2. Cleland JG, Daubert JC, Erdmann E, et al. The effect of cardiac resynchronization on morbidity and mortality in heart failure. N Engl J Med. 2005; 352:1539–1549. [PubMed: 15753115]
3. Auricchio A, Stellbrink C, Block M, et al. Effect of pacing chamber and atrioventricular delay on acute systolic function of paced patients with congestive heart failure. The Pacing Therapies for Congestive Heart Failure Study Group. The Guidant Congestive Heart Failure Research Group. Circulation. 1999; 99:2993–3001. [PubMed: 10368116]
4. Blanc JJ, Etienne Y, Gilard M, et al. Evaluation of different ventricular pacing sites in patients with severe heart failure: results of an acute hemodynamic study. Circulation. 1997; 96:3273–3277. [PubMed: 9396415]
5. Etienne Y, Mansourati J, Gilard M, et al. Evaluation of left ventricular based pacing in patients with congestive heart failure and atrial fibrillation. Am J Cardiol. 1999; 83:1138–1140. A9. [PubMed: 10190537]
6. Thibault B, Ducharme A, Harel F, et al. Left ventricular versus simultaneous biventricular pacing in patients with heart failure and a QRS complex >/=120 milliseconds. Circulation. 2011; 124:2874–2881. [PubMed: 22104549]
7. Gasparini M, Bocchiardo M, Lunati M, et al. Comparison of 1-year effects of left ventricular and biventricular pacing in patients with heart failure who have ventricular arrhythmias and left bundle-branch block: the Bi vs Left Ventricular Pacing: an International Pilot Evaluation on Heart Failure Patients with Ventricular Arrhythmias (BELIEVE) multicenter prospective randomized pilot study. Am Heart J. 2006; 152:155, e1–e7. [PubMed: 16824846]
8. Boriani G, Kranig W, Donal E, et al. A randomized double-blind comparison of biventricular versus left ventricular stimulation for cardiac resynchronization therapy: the Biventricular versus Left Univentricular Pacing with ICD Back-up in Heart Failure Patients (B-LEFT HF) trial. Am Heart J. 2010; 159:1052–1058. e1. [PubMed: 20569719]
9. Leclercq C, Faris O, Tunin R, et al. Systolic improvement and mechanical resynchronization does not require electrical synchrony in the dilated failing heart with left bundle-branch block. Circulation. 2002; 106:1760–1763. [PubMed: 12356626]
10. Prinzen FW, Hunter WC, Wyman BT, McVeigh ER. Mapping of regional myocardial strain and work during ventricular pacing: experimental study using magnetic resonance imaging tagging. J Am Coll Cardiol. 1999; 33:1735–1742. [PubMed: 10334450]
11. Lumens J, Delhaas T, Kirn B, Arts T. Three-Wall Segment (TriSeg) Model Describing Mechanics and Hemodynamics of Ventricular Interaction. Ann Biomed Eng. 2009; 37:2234–2255. [PubMed: 19718527]
12. Leenders GE, Lumens J, Cramer MJ, et al. Septal deformation patterns delineate mechanical dyssynchrony and regional differences in contractility: analysis of patient data using a computer model. Circ Heart Fail. 2012; 5:87–96. [PubMed: 21980078]
13. Lumens J, Leenders GE, Cramer MJ, et al. Mechanistic Evaluation of Echocardiographic Dyssynchrony Indices: Patient Data Combined with Multiscale Computer Simulations. Circ Cardiovasc Imaging. 2012; 5:491–499. [PubMed: 22661491]
14. Strik M, Rademakers LM, van Deursen CJ, et al. Endocardial left ventricular pacing improves cardiac resynchronization therapy in chronic asynchronous infarction and heart failure models. Circ Arrhythm Electrophysiol. 2012; 5:191–200. [PubMed: 22062796]
15. Surawicz B, Childers R, Deal BJ, et al. AHA/ACCF/HRS recommendations for the standardization and interpretation of the electrocardiogram: part III: intraventricular conduction disturbances: a scientific statement from the American Heart Association Electrocardiography and Arrhythmias Committee, Council on Clinical Cardiology; the American College of Cardiology Foundation; and the Heart Rhythm Society. J Am Coll Cardiol. 2009; 53:976–981. [PubMed: 19281930]

16. Derval N, Steendijk P, Gula LJ, et al. Optimizing hemodynamics in heart failure patients by systematic screening of left ventricular pacing sites: the lateral left ventricular wall and the coronary sinus are rarely the best sites. J Am Coll Cardiol. 2010; 55:566–575. [PubMed: 19931364]
17. Ramanathan C, Ghanem RN, Jia P, Ryu K, Rudy Y. Noninvasive electrocardiographic imaging for cardiac electrophysiology and arrhythmia. Nat Med. 2004; 10:422–428. [PubMed: 15034569]
18. Ploux S, Lumens J, Whinnett Z, et al. Noninvasive electrocardiographic mapping to improve patient selection for cardiac resynchronization therapy: Beyond QRS duration and left bundle-branch block morphology. J Am Coll Cardiol. 2013; 61:2435–2443. [PubMed: 23602768]
19. Arts T, Delhaas T, Bovendeerd P, Verbeek X, Prinzen FW. Adaptation to mechanical load determines shape and properties of heart and circulation: the CircAdapt model. Am J Physiol Heart Circ Physiol. 2005; 288:H1943–H1954. [PubMed: 15550528]
20. ter Keurs HE, Rijnsburger WH, van Heuningen R, Nagelsmit MJ. Tension development and sarcomere length in rat cardiac trabeculae. Evidence of length-dependent activation. Circ Res. 1980; 46:703–714. [PubMed: 7363419]
21. Belenkie I, Smith ER, Tyberg JV. Ventricular interaction: from bench to bedside. Ann Med. 2001; 33:236–241. [PubMed: 11405544]
22. Rademakers LM, van Kerckhoven R, van Deursen CJ, et al. Myocardial infarction does not preclude electrical and hemodynamic benefits of cardiac resynchronization therapy in dyssynchronous canine hearts. Circ Arrhythm Electrophysiol. 2010; 3:361–368. [PubMed: 20495014]
23. Martin DO, Lemke B, Birnie D, et al. Investigation of a novel algorithm for synchronized left-ventricular pacing and ambulatory optimization of cardiac resynchronization therapy: results of the adaptive CRT trial. Heart Rhythm. 2012; 9:1807–1814. [PubMed: 22796472]

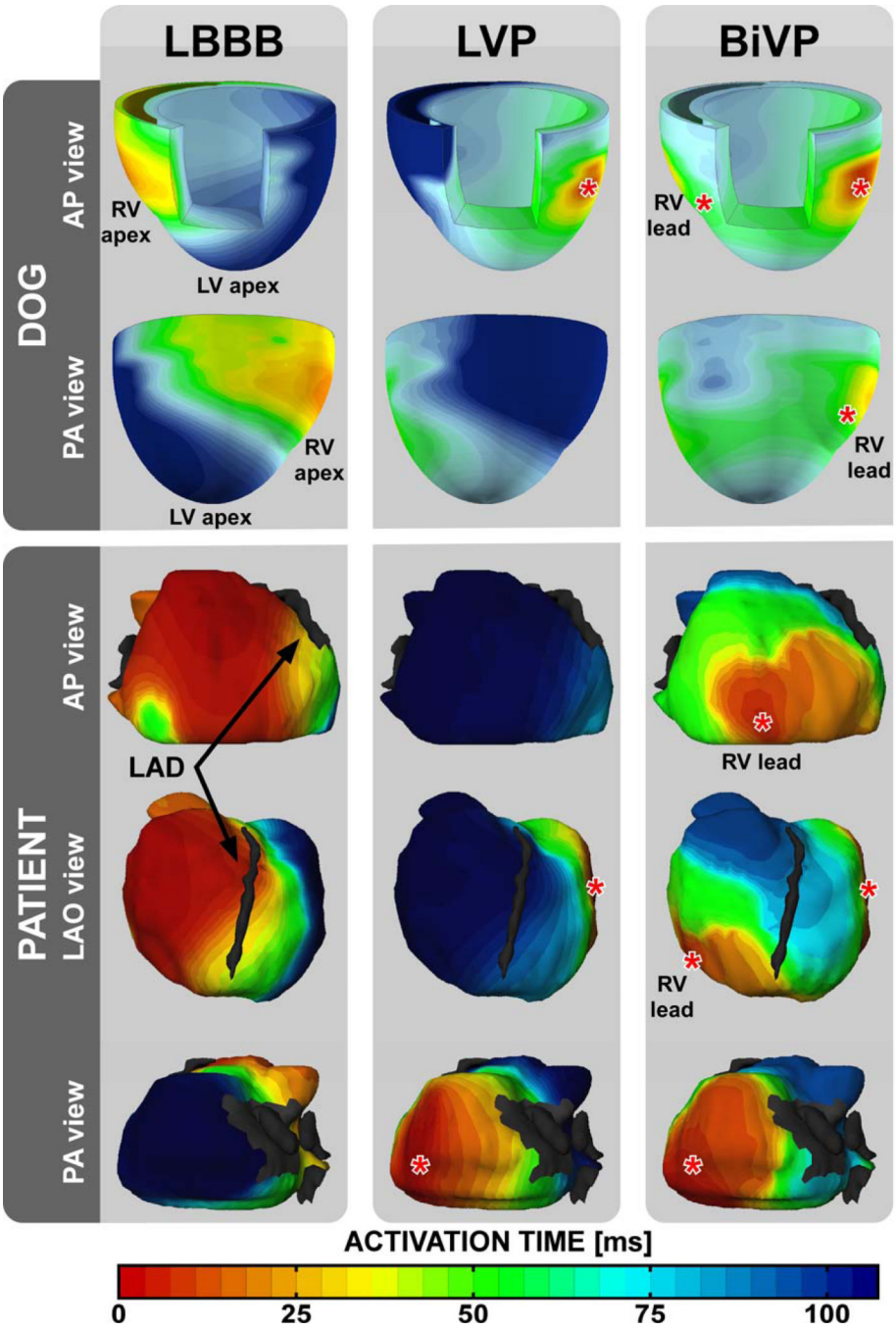

Figure 1. Electrocardiographic mapping in a dog and a patient with nonischemic heart failure and LBBB

Isochronal maps show timing of electrical activation during baseline, LVP, and BiVP. Black arrows indicate the left anterior descending coronary artery (LAD). The gray patch in the PA view represents the segmentation of the mitral orifice. Red asterisks indicate pacing sites. AP = anterior-posterior, LAO = left anterior oblique, and PA = posterior-anterior.

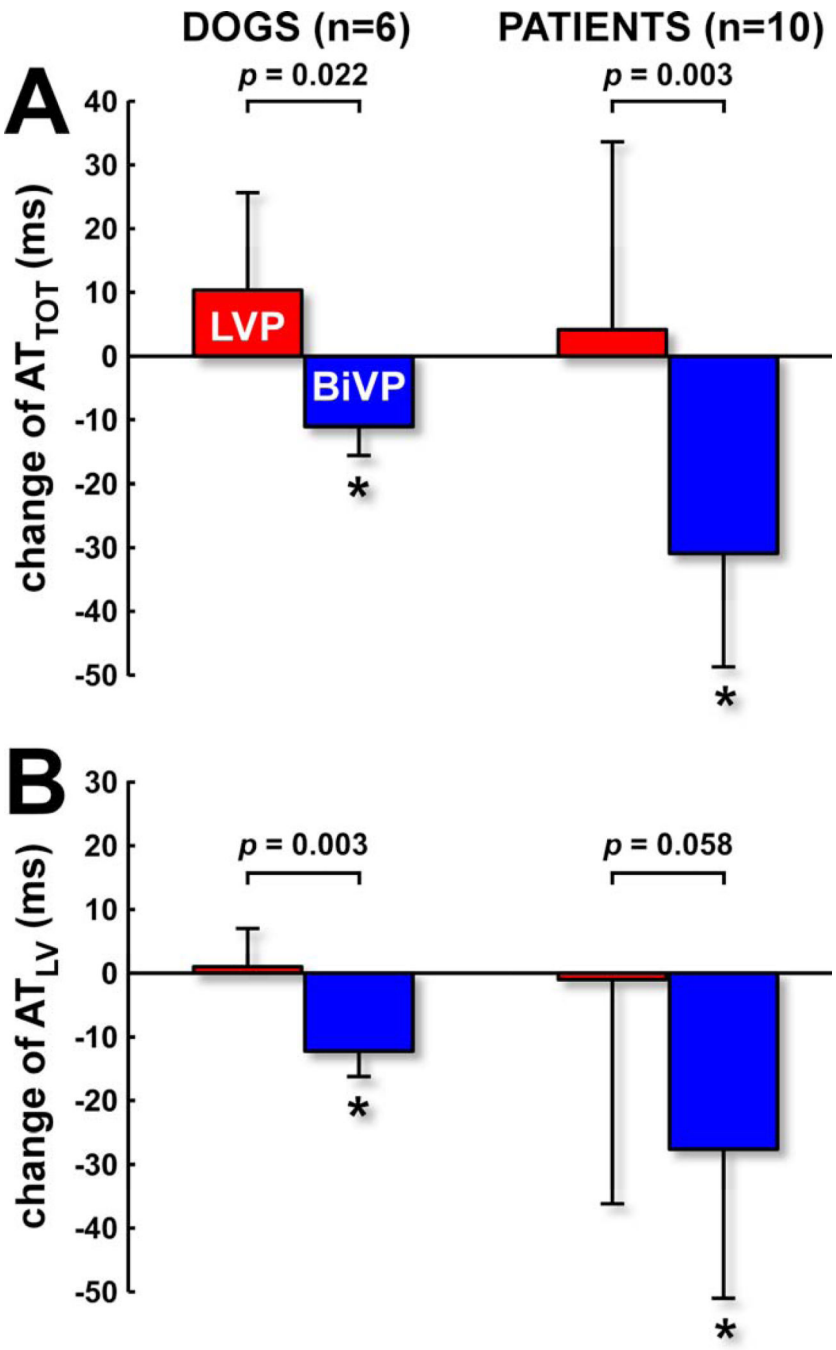

Figure 2. Pacing-induced changes of electrical dyssynchrony in dogs and patients

A) Change of total ventricular activation time (LV+RV free walls+septum in dogs; LV+RV free walls in patients). **B)** Change of LV activation time (LV free wall+septum in dogs; only LV free wall in patients). * $p<0.05$ versus baseline.

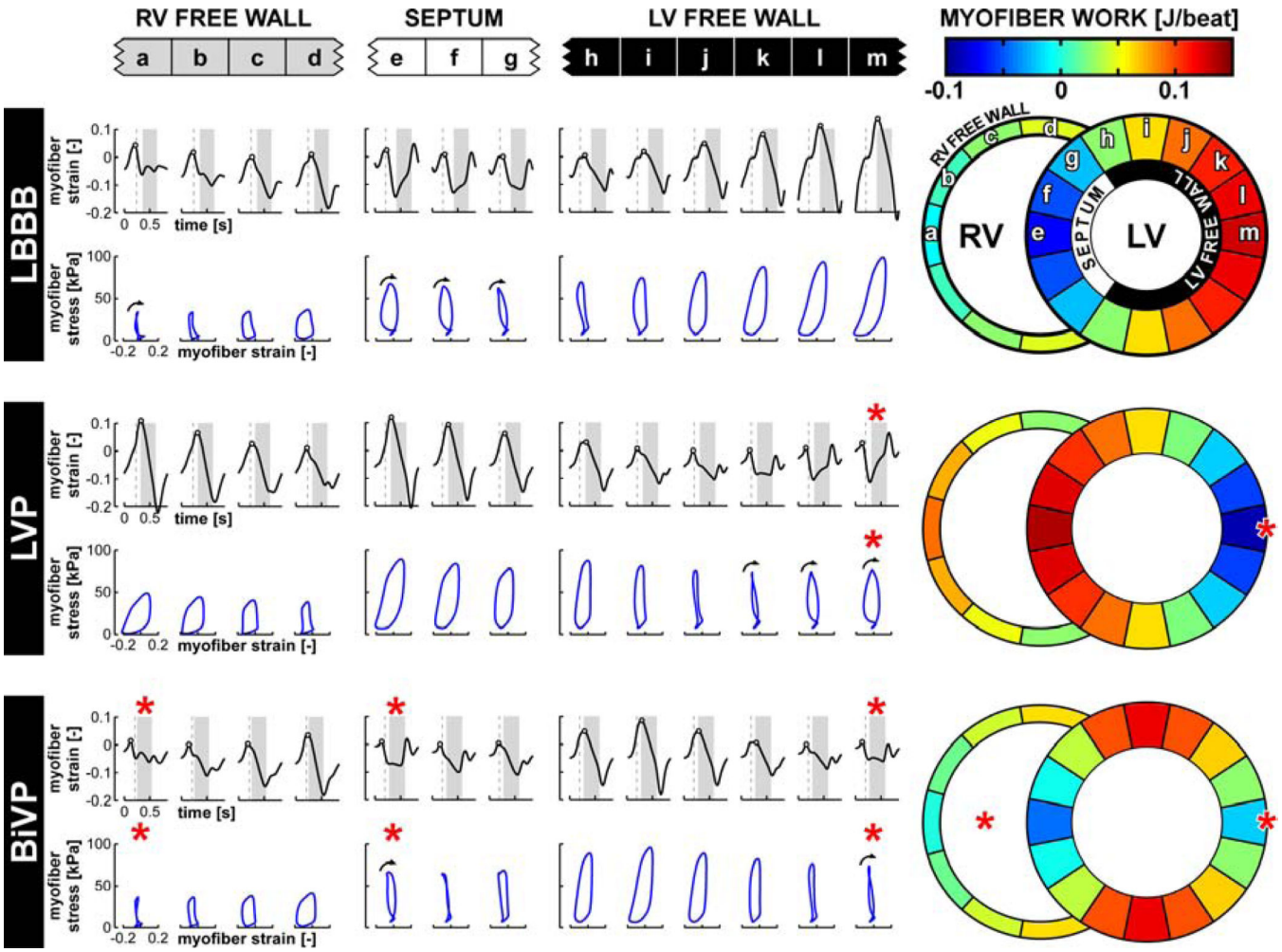

Figure 3. Simulated local myofiber mechanics in a failing heart during LBBB and pacing

Time courses of natural myofiber strain are plotted in black. Red asterisks indicate pacing sites. Vertical dashed lines indicate moment of mitral valve closure and LV ejection is highlighted in grey. Black circles indicate onset of systolic shortening. Relations between myofiber stress and myofiber strain are plotted in blue. Black arrows indicate segments with a clockwise stress-strain relation, indicating negative myofiber work. Color maps indicate myofiber work per ventricular wall segment.

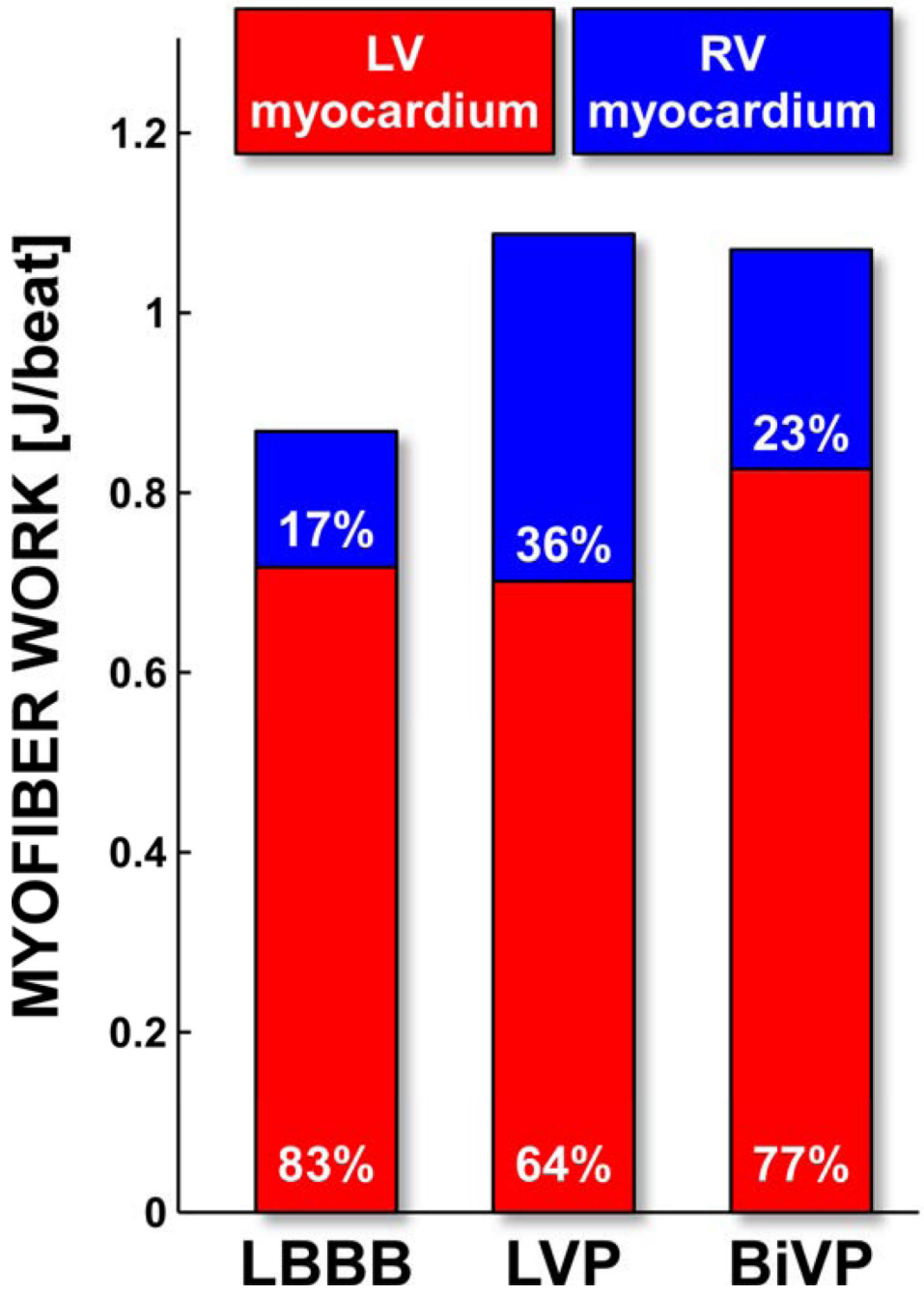

Figure 4. Distribution of ventricular myofiber work during LBBB and pacing

Total ventricular myofiber work generated per cardiac cycle; percentages indicate the relative contributions of the LV and RV myocardium. LV myocardium includes the interventricular septum and the LV free wall.

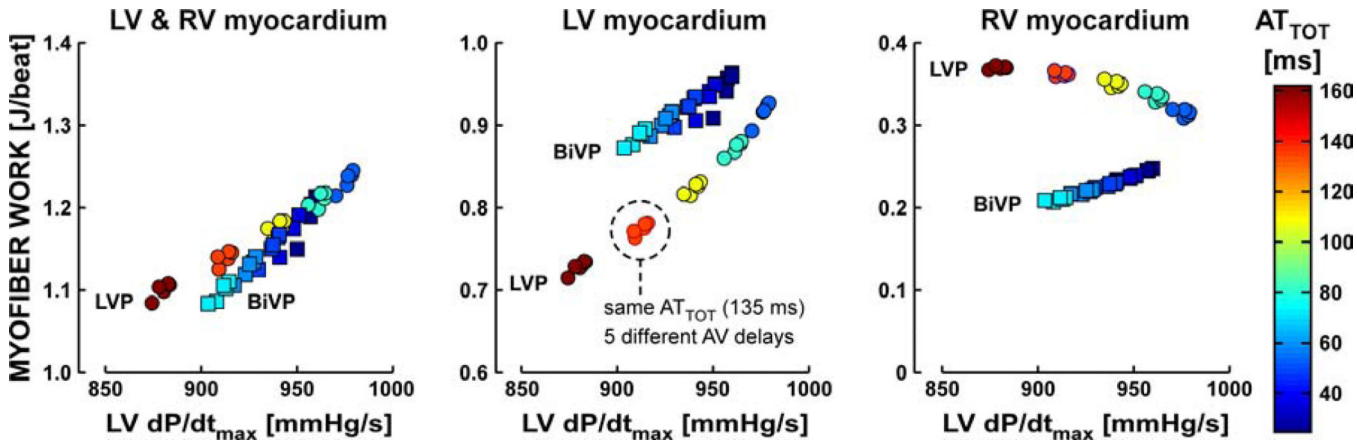

Figure 5. Relationship between ventricular myofiber work and LV systolic function during pacing

Total ventricular myofiber work (left), LV myofiber work (middle), and RV myofiber work (right) per cardiac cycle versus LVdP/dt$_{max}$ in 25 LVP simulations (circles) and 25 BiVP simulations (squares). The left panel indicates that total ventricular myofiber work increased linearly with LVdP/dt$_{max}$ and that this linear relationship was virtually independent of the pacing mode. The middle and right panel show that LVP and BiVP behaved differently when considering LV and RV myofiber work separately. For both pacing modes, five clusters of simulations can be discriminated by their color, indicating total ventricular activation time (AT$_{TOT}$) that ranged from 54 to 162 ms for LVP and from 24 to 72 ms for BiVP. Each cluster (e.g. dashed circle) consists of five simulations with the same AT$_{TOT}$, but with different AV delays (60/80/100/120/140 ms).

Table 1

Electrical and hemodynamic data from dogs with chronic HF and LBBB (n=6) during baseline (BL), left ventricular pacing (LVP), and biventricular pacing (BiVP).

				p-values			
	BL	**LVP**	**BiVP**	**ANOVA**	**BL vs LVP**	**BL vs BiVP**	**LVP vs BiVP**
QRS duration (ms)	122±10	132±26	115±15	0.098	-	-	-
heart rate (bpm)	134±11	133±10	133±10	0.368	-	-	-
AT_{TOT} (ms)	95±16	106±22	84±13	0.008	0.160	**0.002**	**0.022**
AT_{LV} (ms)	95±16	96±14	83±13	<0.001	0.701	**0.001**	**0.003**
LV stroke volume (mL)	15±5	17±11	18±7	0.428	-	-	-
LV pump stroke work (mL*mmHg)	1022±503	1245±883	1230±499	0.256	-	-	-
LV peak systolic pressure (mmHg)	77±11	79±10	79±10	0.105	-	-	-
$LVdP/dt_{max}$ (mmHg/s)	853±99	1023±158	1005±127	0.034	**0.038**	**0.035**	0.295
LV end-diastolic pressure (mmHg)	20±13	19±14	21±15	0.279	-	-	-
LV end-diastolic volume (mL)	128±37	124±36	127±35	0.223	-	-	-
RV peak systolic	32±12	29±11	31±11	0.015	**0.026**	0.155	0.053
pressure (mmHg) $RVdP/dt_{max}$ (mmHg/s)	442±140	411±146	463±118	0.050	0.136	0.290	**0.043**
RV end-diastolic pressure (mmHg)	8±6	8±4	9±7	0.894	-	-	-

AT_{LV} = LV electrical activation time (including septum and LV free wall); AT_{TOT} = total ventricular electrical activation time (including septum, LV free wall, and RV free wall).

J Am Coll Cardiol. Author manuscript; available in PMC 2014 December 24.

Table 2

Baseline patient characteristics.

	All patients (n=24)	ECM subgroup (n=10)
Age (yrs)	66±12	66±12
Male gender	17 (71%)	8 (80%)
NYHA functional class		
II	7 (29%)	4 (40%)
III	17 (71%)	6 (60%)
Ischemic etiology	8 (33%)	3 (30%)
QRS duration (ms)	164±22	162±24
PR interval (ms)	213±30	225±37
LV ejection fraction (%)	27±3	26±5

Data are presented as mean±SD or as absolute numbers with percentage of total population in parentheses.

Table 3

Electrical and hemodynamic patient data during baseline (BL), left ventricular pacing (LVP), and biventricular pacing (BiVP).

				p-values			
	BL	**LVP**	**BiVP**	**ANOVA**	**BL vs LVP**	**BL vs BiVP**	**LVP vs BiVP**
All patients (n=24)							
$LVdP/dt_{max}$ (mmHg/s)	728±221	844±281	838±250	<0.001	**<0.001**	**<0.001**	0.687
ECM subgroup (n=10)							
$LVdP/dt_{max}$ (mmHg/s)	737±204	827±251	822±238	<0.001	**0.006**	**0.001**	0.666
AT_{TOT} (ms)	130±12	131±26	96±14	0.004	0.915	**0.001**	**0.014**
AT_{LV} (ms)	112±26	105±15	89±18	0.099	-	-	-

AT_{LV} = LV epicardial electrical activation time (including septum and LV free wall); AT_{TOT} = total epicardial electrical activation time (including septum, LV free wall, and RV free wall); BiVP = biventricular pacing; BL = Baseline; LVP = left ventricular pacing.

Table 4

Electrical and hemodynamic data derived from computer simulations of a failing heart during baseline (BL), left ventricular pacing (LVP), and biventricular pacing (BiVP).

	BL	LVP	BiVP
heart rate (bpm)	80	80	80
AV delay (ms)	220	100	100
AT_{TOT} (ms)	135	135	60
AT_{LV} (ms)	120	120	60
LV stroke volume (mL)	53	61	62
LV pump stroke work (mL*mmHg)	4911	6289	6363
LV peak systolic pressure (mmHg)	113	128	127
$LVdP/dt_{max}$ (mmHg/s)	710	815	818
LV end-diastolic pressure (mmHg)	19	24	25
LV ejection fraction (%)	23	25	25
RV pump stroke work (mL*mmHg)	1641	1913	1906
RV peak systolic pressure (mmHg)	36	36	36
$RVdP/dt_{max}$ (mmHg/s)	328	270	290
RV end-diastolic pressure (mmHg)	5	5	6

AT_{LV}, LV electrical activation time (including septum and LV free wall); AT_{TOT}, total ventricular electrical activation time (including septum, LV free wall, and RV free wall).